International Journal of Research and Engineering
ISSN: 2348-7860 (O) | 2348-7852 (P) | Vol. 04 No. 09 | September 2017 | PP. 244-250

Speed Control of Parallel Connected DSIM Fed by Six Phase Inverter with IFOC Strategy Using ANFIS

Author(s): M AnkaRao [1], Dr. M Vijayakumar[2], N Premanath Kumar [3]
[1] Assistant Professor, [2]Professor, Dept.of Electrical Engineering, [3] PG Scholar,
Dept.of Electrical Engineering, JNTUA College of Engineering, Ananatapur, Andhra Pradesh, India.

Abstract: **This paper describe the presentation of an IM for high load and high-power applications, this kind of applications the motor have a complex coupling between the field and torque. This can be achieve with assist of Indirect Field Oriented Control (IFOC) and parallel connection of two motors. The benefit is that parallel connection can provide the decoupled control of flux and torque for each motor and their concert in different operating environments. The Speed control of two Double Star Induction Motors working in parallel configuration with IFOC using a Fuzzy Logic Controller (FLC) and Adaptive Neuro Fuzzy Inference (ANFIS) controller is investigate in different operating environments. The two motors are connected in parallel at the output of a single six-phase PWM based inverter fed from a DC source. Performance of the projected method under load disturbances is studied through simulation using a MATLAB and e valuation of speed response of two controllers is analyzed.**

Key terms: Double Star Induction Motor (DSIM), Fuzzy logic controller (FLC), Indirect Field Oriented Control (IFOC), Adaptive Neuro Fuzzy Inference (ANFIS), and Six Phase Inverter.

I. INTRODUCTION

In the industrialized applications where high reliability is demanded, multi-phase induction machine is used instead of 3-phase IM. The DSIM is being used in many applications, but the main complexity to control this machine resides in the fact that complex coupling exists between the field and the torque. The field-oriented control (FOC) technique has been proposed in industry for high performance induction machine drive. The control aim is to produce a decoupled control of the flux and the torque of the machine. This method is being applied to conventional three-phase IM, but its purpose is to encourage a multi phase machine for high-power applications. A DSIM drive, particularly for high-power applications, has been increased considerably over the years [1-4]. This kind of machine is composed of two windings with a 30-electrical degree phase shift. These windings are normally fed by a six-phase inverter supply in VSD [3, 4-7]. With this major advantages, the drive method with two Double Star Induction Motors working in parallel and fed by a single PWM based SPVSI can be used in some applications particularly in the field of high power electric/hybrid vehicles, rolling stock traction system such as locomotive and electric ship propulsion [1-3,5,8-10]. The major advantages of this motor are:

1. Reduction in torque ripple.
2. Reduction of rotor harmonics as they can be filtered.
3. DC-link current harmonics can be reduced.
4. This machine works when the one or more phases in fault.[1-4, 7, 8, and 10].

In current years, various parallel configurations has been projected for two multi-phase machines drive to feed them from a single VSI [4,11-17]. Among multi-phase machines; 5-phase and 6-phase machines are more common. A parallel configuration to feed two 5-phase motor from a single VSI is recommended in [11], and a sliding mode control based speed control of two 6-phase motors connected in parallel to a single VSI supply is projected in [4]. These parallel configurations offer a decoupled control of flux and torque and each machine performance is evaluated experimentally. Speed control of indirect field oriented controlled DSIMs connected in parallel to a single SPVSI supply using FLC and ANFIS is investigated. This kind system is suitable for applications using dual DSIMs with the benefit of compactness, weightlessness and economy [12].Though, the control performance of the DSIM is still influenced by the parameters variations in motor, particularly the rotor time constant. Against this disadvantage, we presented a robust control technique based on ANFIS logic. For this reason, in order to make the control system insensitive to parameter variations, this study is to design a suitable control scheme IFOC DSIM drive where the stator voltage waveforms are generated by SPVSI. FLC and ANFIS have been effectively used for a small number of numbers of nonlinear and complex processes. The FLC and ANFIS are robust and their performance is insensitive to the parameter variations contrary to conventional regulators. Against this disadvantage, we suggest a robust control method based on fuzzy logic. For this, the FLC has been suggested to achieve robust performance of indirect field-oriented control.

II. SYSTEM CONFIGURATION

A diagram of the IFOC of dual motors connected in parallel to a SPVSI supply is shown in Fig. 1. This method has been adopt in order to avoid the over magnetization of these motors. This technique is characterized by the slip angular speed calculation, the stator flux angle calculation and the rotor angular speed calculation. Two DSIMs speeds are measured using sensors. The torque reference of each DSIM is calculated by the difference between reference speeds. FLC and ANFIS controllers are used in the speed control loops for the DSIMs as shown in the Fig.1. The other block in the fig can be found in the conventional field vector control technique [1]. Study of the drive system in the PWM mode in the middle speed region and in the single pulse mode in the high-speed region is performed. The robustness of the projected technique is checked in terms of motor speed and load fluctuations.

III. DSIM MODLEING

Equations used to model each DSIM in the Park reference frame are

Stator and Rotor voltage Equations are:

$$V_{ds1} = Rs\, I_{ds1} + P\lambda_{ds1} - Ws\lambda_{qs1} \quad (1)$$

$V_{ds2}= Rs\ I_{ds2} + P\lambda_{ds2} - Ws\lambda_{qs2}$ (2)
$V_{qs1}= Rs\ I_{qs1} + P\lambda_{qs1} + Ws\lambda_{ds1}$ (3)
$V_{qs2}= Rs\ I_{qs2} + P\lambda_{qs2} + Ws\lambda_{ds2}$ (4)
$0= Rr\ I_{qr} + P\lambda_{qr} + (Ws-Wr)\ \lambda_{dr}$ (5)
$0= Rr\ I_{dr} + P\lambda_{dr} - (Ws-Wr)\ \lambda_{qr}$ (6)

Stator and Rotor flux linkages equations are:
$\lambda_{ds1} = Ls\ I_{ds1} + Lm\ (I_{ds1}+I_{ds2}+I_{dr})$ (7)
$\lambda_{ds2} = Ls\ I_{ds2} + Lm\ (I_{ds1}+I_{ds2}+I_{dr})$ (8)
$\lambda_{qs1} = Ls\ I_{qs1} + Lm\ (I_{qs1}+I_{qs2}+I_{qr})$ (9)
$\lambda_{qs2} = Ls\ I_{qs2} + Lm\ (I_{qs1}+I_{qs2}+I_{qr})$ (11)
$\lambda_{dr} = Lr\ I_{dr} + Lm\ (I_{ds1}+I_{ds2}+I_{dr})$ (12)

An electromagnetic torque equation of DSIM is:
$T_e = \frac{Pm\ Lm}{Lm + Lr}\ [(I_{qs1} + I_{qs2})\ \lambda_{dr} - (I_{ds1} + I_{ds2})\ \lambda_{qr}]$ (13)
Mechanical equation of each DSIM is:
$T_{em-M} - T_{L-M} = J\ P\ \Omega_M + K_f \Omega_M$ (14)
where W_s is the synchronous reference frame; L_s and L_r are stator and rotor inductances, respectively; L_m is the mutual inductance; P_M is the no. of pole pairs; J is the moment of inertia; k_f is the viscous friction coefficient; T_{L-M} is the load torque; W_{r-M} is the rotor electrical angular speed; Ω is the rotor mechanical angular speed, and M denotes DSIM-1 or DSIM-2.All of these parameters are for each of the two DSIMs. The currents, i_{s1} and i_{s2}, flowing in each motor can be expressed by i_s which flows equally in both motors, and i_{s1} and i_{s2} which circulates between the two motors. Currents flowing in the parallel connected DSIMs are shown in Fig.3 and the association of these currents is given below:

$i_{s1} = is_1^{ml} + is_1^{m2}$, $i_{s2} = is_2^{ml} + is_2^{m2}$
$\Delta Is1 = \frac{is1m2 - is1ml}{2}$ And $\Delta Is2 = \frac{is2m2 - is2ml}{2}$

IV. DUAL DSIM'S FIELD ORIENTED CONTROL

A. Reference-Frame:

By selecting the orientation of the rotor flux linkage, the electromagnetic torque and rotor flux linkage will be linked directly to the stator current components. Assume the rotor flux linkages are aligned with the d-axis:
$\lambda_{dr} = \lambda r^*$ (15)
$\lambda_{qr} = 0$ (16)
Thus, $\lambda r^* = \frac{\lambda r1^* + \lambda r2^*}{2}$
Where $\lambda r1^*$ and $\lambda r2^*$ are Flux linkages.

B. Control Strategy:

The reference voltages (V_{ds1}^*, V_{qs1}^*, $Vds2^*$ and V_{qs2}^*) are derived by substituting Eqs. (15) and (16) in Eqs. (1) - (4).
$V_{ds1}^* = RsI_{ds1} + L_sPI_{ds1} - Ws^*(L_s\ I_{qs1} + W_{sl}^*\ T_r\lambda r^*)$ (17)
$V_{qs1}^* = RsI_{qs1} + L_sPI_{qs1} - Ws^*(L_sI_{ds1} + \lambda r^*)$ (18)
$V_{ds2}^* = RsI_{ds2} + 1\ L_sPI_{ds2} - Ws^*(L_sI_{qs2} + W_{sl}^*\ T_r\lambda r^*)$ (19)
$V_{qs2}^* = Rs\ I_{qs2} + L_s\ P\ I_{qs2} - Ws^*\ (L_s\ I_{ds2} + \lambda r^*)$ (20)
Where, P=d/dt
$I_{ds1} = i_{ds1}^{ml} + i_{ds1}^{m2}$, $I_{ds2} = i_{ds2}^{ml} + i_{ds2}^{m2}$,
$I_{qs1} = i_{qs1}^{ml} + i_{qs1}^{m2}$ and $I_{qs2} = i_{qs2}^{ml} + i_{qs2}^{m2}$.
$T_r = L_r / R_r$ (21)
T_r denotes a rotor time constant.

The component of reference of Stator current and slip speed can be expressed as
$Wsl^* = \frac{Rr + Lm}{(Lr + Lm)\ \lambda r^*} I_{qs}^*$ (22)
$I_{ds}^* = \lambda r^* / L_m$ (23)
$Iqs^* = \frac{Lr + Lm}{P\ Lm\lambda r^*} Tem^*$ (24)

The d–q axes currents are referred as flux-producing I_{ds}^* and torque-producing I_{qs}^* components of the DSIMs' stator currents, respectively. To generate the reference voltage vectors (V_{ds1}^*, V_{qs1}^*, $Vds2^*$ and V_{qs2}^*) we are introducing a PI controller in Fig.2.

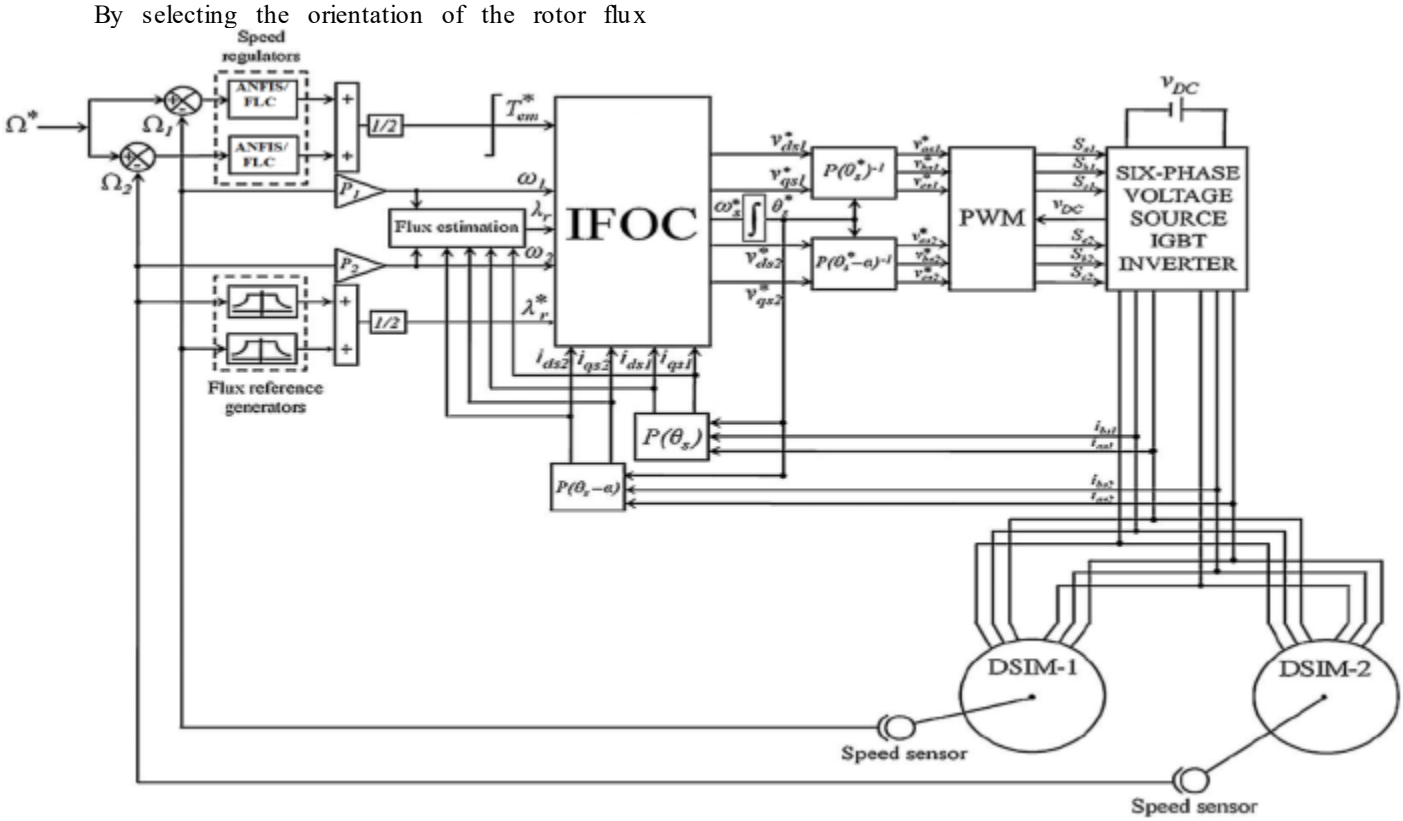

Fig.1. Block diagram of the indirect field oriented control.

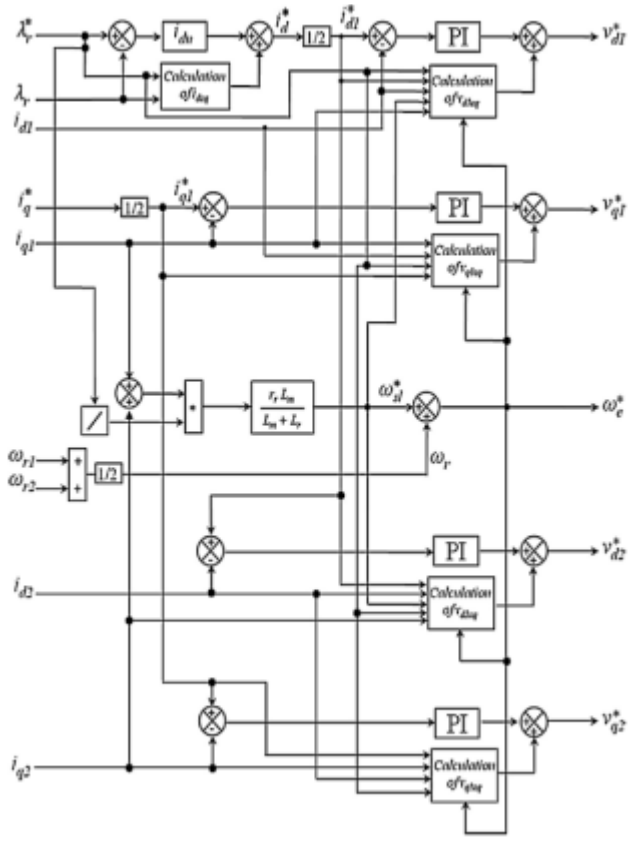

Fig.2. IFOC of the DSIMs.

E_N	Ecn	A_{nb}	A_{pb}
B_{nb}		U_{nb}	U_{ze}
B_{pb}		U_{ze}	U_{pb}

Fig.3. Current flows for parallel connected dual DSIM's.

V. FUZZY CONTROLLER:

This FLC theory is based on the approach of expert data to take the decision. FLC is proposed in Fig.4. FLC is an interesting choice to the traditional controllers such as PI, P and PID etc. This may not yield fully acceptable control performance if the controlled dynamic plant is highly non-linear, uncertain and operates over a wide range [18]. FLC using the product-sum-gravity inference technique consists of four blocks: fuzzification, knowledge base, inference mechanism and deffuzification [5]. The input variables of FLC are the error, E_N, and changes in error, E_{CN}, signals. The output variable is generated from fuzzy rule base and product-sum-gravity method. After the control is computed, defuzzifier is used to obtain the crisp signal. The speed error and error change signals are defined as:

$$E(k) = \Omega_{ref}(k) - \Omega(k) \quad (25)$$

$$E_c(k) = E(k) - E(k-1) \quad (26)$$

Where Ω represent the rotor mechanical angular speed. The corresponding output (U_f) is the torque constituent T_{em-M}.

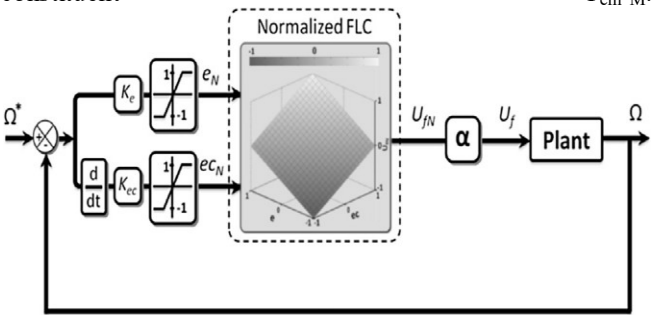

Fig.4. Fuzzy logic controller.

The inputs and the output are related as:

$$U_{fN}(t) = f(e(t), ec(t)) \quad (27)$$

The association between scaling factors and the input and out-put variables of the controller are as follows

$E_N = K_e E$, $Ec_N = K_{ec} Ec$ and $U_f = U_{fN}$

The scaling factor (SFs) K_e and K_{ec} are used to normalize the error E (t) and error changes E_c (t), correspondingly. Notice that the normalized inputs, (E, E_c), remain within the limits of −1 to +1.The product sum gravity method is shown [20] Fig.5 and fuzzy rules has the form [19, 20] table 1

Table 1. Fuzzy rules.

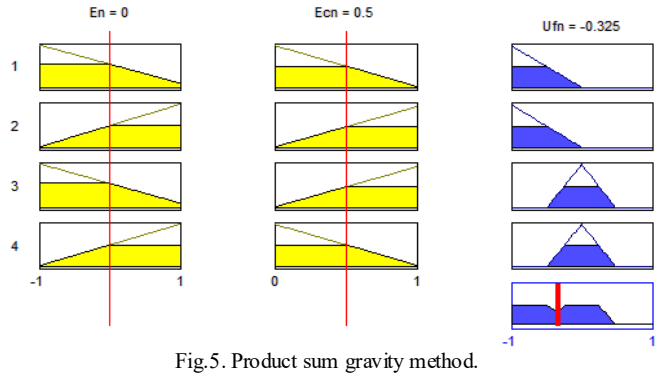

Fig.5. Product sum gravity method.

Where A_i, B_i is the membership functions (MFs) of E_N and Ec_N, correspondingly, and U_{fN} is MF of the output variable of the fuzzy controller.

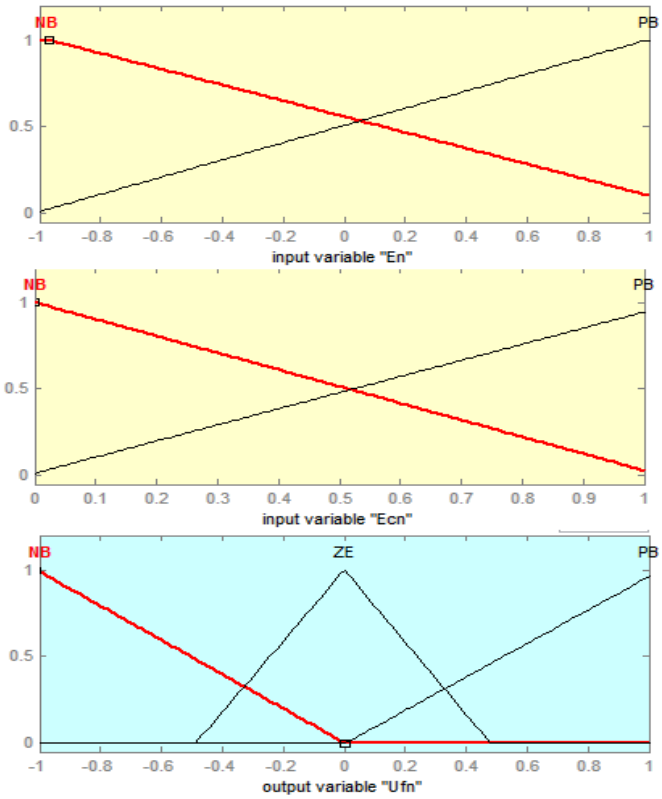

Fig.6. Membership functions of input and output variables.

The MFs used for input and output fuzzy sets are shown in Fig.6 and in the next stage, after computing the inputs through knowledge base and inferencing mechanism is that of de-fuzzification. Here in this paper the deffuzification technique chosen is the center of gravity. Then, the control output U_{fN} can be calculated as follows:

$$U_{fN} = \frac{\sum_{k=1}^{4} \mu(U_{fN}(K))\, U_{fN}(K)}{\sum_{K=1}^{4} \mu(U_{fN}(K))} \quad (28)$$

Here $\mu(U_{fN}(k))$ is the output membership value for k^{th} rule and $U_{fN}(k)$ represents the output value of FLC. The linear control surface of output (U_{fN}) of the FLC controller based on only four rules is shown Fig.7 w.r.to product-sum-gravity (PSG) method.

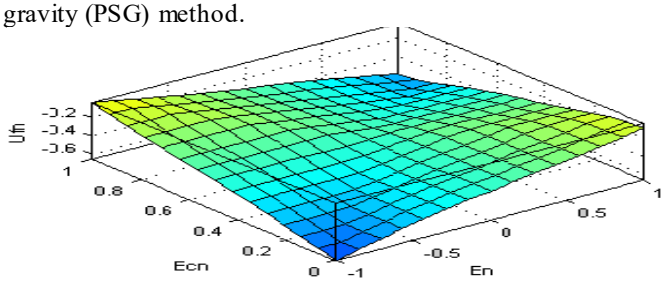

Fig.7. Control surface of FLC controller.

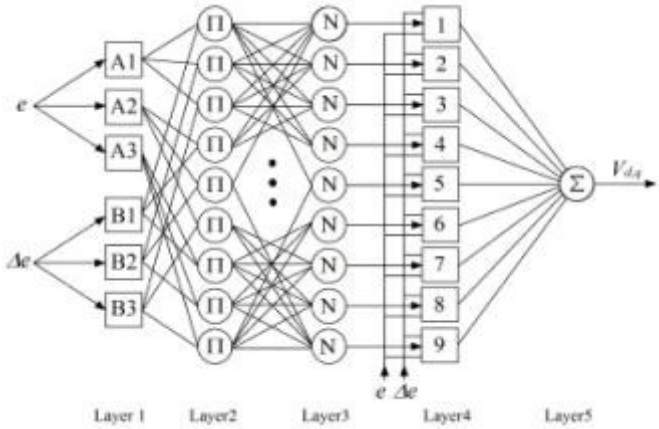

VI. ANFIS CONTROLLER

ANFIS is an intelligent system and is proved to be efficient in problems similar to categorization, modeling, and control of complex systems. ANFIS are realized by an suitable combination of neural and fuzzy systems. The premise parameters and consequent parameters are tuned with the help of back-propagation algorithm. The projected neuro fuzzy controller incorporates fuzzy logic algorithm with a five layer artificial neural network (ANN) structure as shown in [21, 22] Fig.8. ANFIS design that has two inputs e and Δe and one output V_d.

Layer 1: This layer is fuzzification layer. Degrees of MF's are calculated in this layer for each input variable. The input variables of ANFIS are chosen as the error (e) and the change of error (Δe) is given by Equation 29 and 30. Every node i in this layer is an adaptive node with node function:

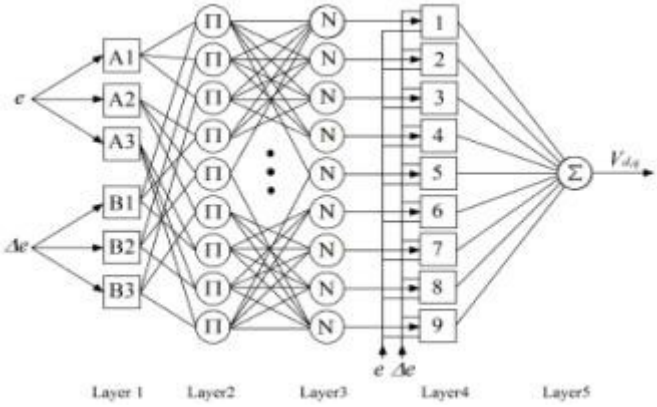

Fig.8. ANFIS structure.

$$e = i_{d\text{-}q}^{*} - i_{d\text{-}q} \quad (29)$$

$$\Delta e = e(k) - e(k-1) \quad (30)$$

$$X = e(t) \quad (31)$$

$$Y = \Delta e(t) \quad (32)$$

$$O_i^1 = \mu_{Ai}(x) = \frac{1}{1+\left[\frac{x-c_i}{a_i}\right]^{b_i}} \quad i = 1,2,3 \ldots \quad (33)$$

$$O_{i+2}^1 = \mu_{Bi}(y) = \frac{1}{1+\left[\frac{y-c_{i+2}}{a_{i+2}}\right]^{b_{i+2}}} \quad i = 1,2,3.. \quad (34)$$

Where, $\{a_i, b_i, c_i\}$ is the parameter set and A is the linguistic term. Bell-shaped MF's is selected for each node.

Layer 2: This layer is rule inference layer. Every node in this layer is a fixed node label as $\prod$ which multiplies the incoming signals and sends the product out. Each node output corresponds to the firing strength of a fuzzy rule.

$$O_i^2 = w_i = \mu_{Ai}(x)\mu_{Bi}(y) \quad i = 1,2,3 \ldots \quad (35)$$

Layer 3: This is a normalization layer. Every node in this layer is a circle node labeled N. The *i-th* node calculates the ratio of the rule's firing strength to the sum of all rules' firing strength.

$$O_i^3 = \bar{w}_i = \frac{w_i}{\sum_i w_i} \quad i = 1,2,3 \ldots \quad (36)$$

Layer 4: This is a consequent layer. All nodes are an adaptive mode with node function:

$$O_i^4 = \bar{w}_i f_i = w_i(p_i x + q_i y + r_i) \quad i = 1,2,3 \ldots \quad (37)$$

Where ANFIS is a normalized firing strength from layer 3, and $\{p_i, q_i, r_i\}$ is the parameter set of this node.

Layer 5: This is output layer. The single node in this layer is a fixed and node is labeled as $\sum$ that computes the overall output as the summing up of all incoming signals:

$$O_i^5 = \sum_i \bar{w}_i f_i \quad i = 1,2,3 \ldots$$

The parameters of ANFIS are updated using the back propagation error term as follow

$$\frac{\partial E}{\partial O^5} = K_1 e + K_2 \Delta e$$

The error (e) and the change of error (Δe) multiplied by the constants k_1 and k_2.

$$\alpha_{K+1} = \alpha_K - \eta \frac{\partial E}{\partial \alpha_K}$$

Where α is any of the parameters of ANFIS and η is learning rate. The error will be reduced next training iteration. The advantage of using ANFIS over a FLC controller is the output MF's is automatically tuned and it can provide better performance than FLC.

VII SIMULATION RESULTS AND DISCUSSION

In order to show the feasibility of the projected FLC and ANIFS controllers, simulation study of the drive system based on the DSIMs in Fig.1.were carried out using MATLAB. Here each DSIM is rated at 5.5 kW and parameters used in the simulation study are shown in Table2. Comparative performance with FLC and ANFIS controllers for tests performed under the same conditions is studied. The response of each DSIM is observed under different operating environments such as a step change in the reference speed or sudden changes in the load. Results of a set of tests of step changes in speed reference are shown in Fig.9 and 10 for the two motors. Variation in the reference speeds of the motors is chosen as (t € [0 0.4] sec, Ω = 50 rad/s) and (t [0.4 3] sec, Ω= 100 rad/s). In these tests the performance of the two controllers is evaluated in terms of speed response. It can be observed that amplitude of transient oscillations of speed is lower with ANFIS which also has better rejection of perturbations. The result shows that the ANFIS controller shows improvement, albeit small, in performance compared to that with the FLC controller. The predictable speeds deviate from the speed references when the conditions of the each DSIM are different.

Steady-state errors in speed and electromagnetic torque variations are interrelated due to the motors are being connected in parallel and there being coupling terms between the d-q axes of each motor. The influence of the step changes in load reference on electromagnetic torque of each motor is shown in Fig.11 and 12. lastly, the simulation results of the DSIMs connected in parallel associated to IFOC using FLC and ANFIS controllers were also analyzed concerning a load torques and speed variations. These results confirm that the ANFIS controller demonstrate a somewhat better performance under changing operating environments and present satisfactory performance. Fig.9 through 12 represents the first 0.4 s show the response to change in speed reference and after 1.0 s the response to change in load reference.

Table2. Motor parameters used in simulation.

Parameter	Symbol and magnitude
Rated voltage	V_r = 220v
Rated current	I_r = 6A
Rated speed	N_r = 1000rpm
Number of poles	P = 6
Frequency	F = 50hz
Stator resistance	Rs = 2.03ohm
Rotor resistance	Rr = 3ohm
Stator inductance	Ls = 0.0147H
Rotor Inductance	Lr = 0.0147H
Mutual inductance	Lm = 0.2H
Moment of inertia	J = 0.06 Kg m^2
Coeff. of Viscous Friction	Kf = 0.006 N ms/rd

From the results, we analyzed the data statistics of DSIMs. That can be shown in table3. From the table ANFIS has good performance compared to FLC because its mean values are near to the reference signal values.

Table 3. Mean values of Load and Speed.

Reff. Signal	FLC	ANFIS
Mean of Wr = 93.36	90.42	91.1
Mean of Te = 8.321	8.33	8.325

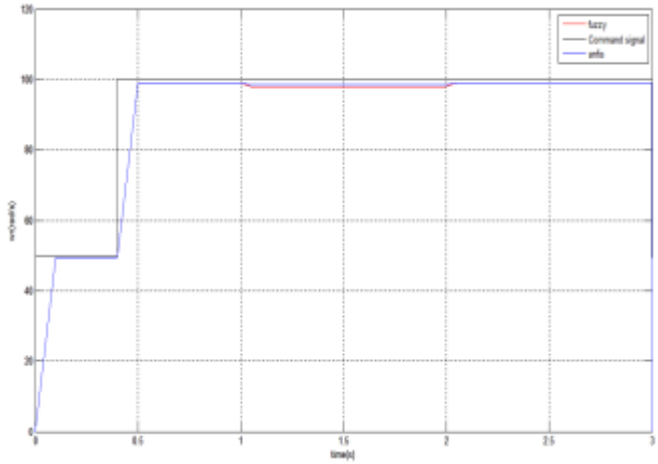

Fig.9. Speed response of DSIM-1

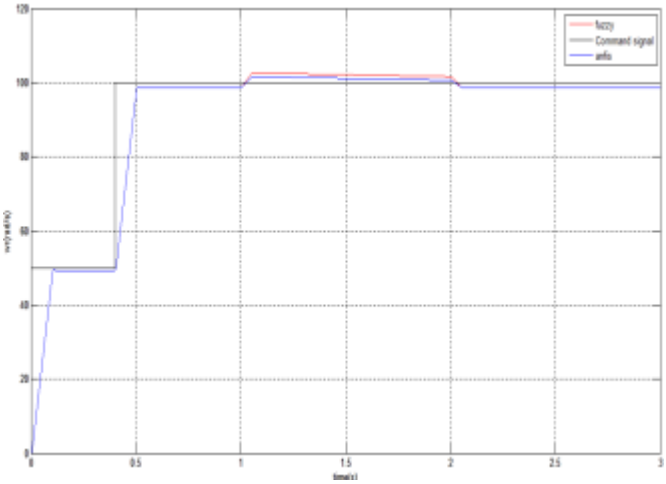

Fig.10. Speed response of DSIM-2

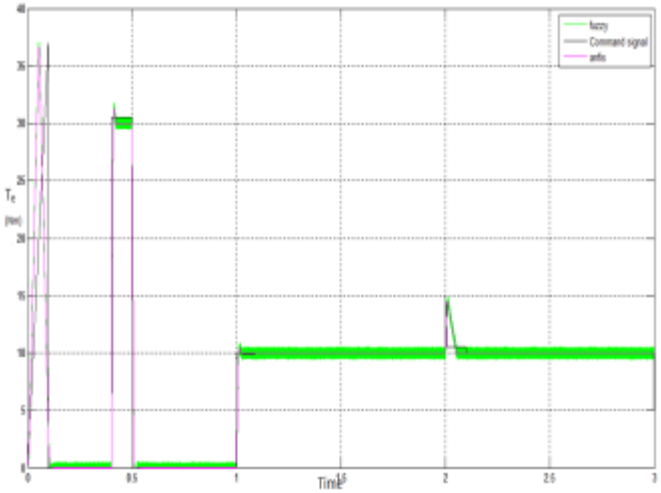

Fig.11. Load response of DSIM-1

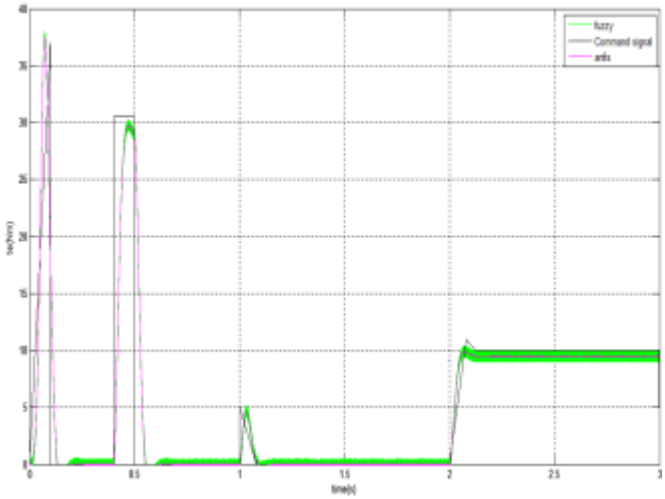

Fig.12. Load response of DSIM-2.

CONCLUSION

Comparison of the performance of two IFOC controlled DSIM's in parallel to a single SPVSI supply using FLC and ANFIS based speed control is presented. It is observed that in terms of speed reference tracking of the dual DSIMs, ANFIS gives a better performance compared to the FLC controller. When the two motors speed is modified, the impact on the electromagnetic torque of the motors is important. The results presented show that the ANFIS controller with only nine rules can provide an effective solution for devices using DSIMs in parallel such as electric/hybrid vehicles, traction locomotives, rolling stock traction system and electric propulsion ships.

REFERENCES

[1] R. Bojoi, M. Lazzari, F. Profumo, A. Tenconi, Digital field-oriented control for dual three-phase induction motor drives, IEEE Trans. Ind. Appl. 39 (May/June

[2] D. Foito, J. Maia, V. Fernao Pires, J.F. Martins, Double three-phase induction machine modeling for internal faults simulation, Electr.Power Compon. Syst.

[3] G.K. Singh, Multi-phase induction machine drive research—a survey, Electr. Power Sys. Res. 61.

[4] N.R. Abjadi, Sliding-mode control of a six-phase series/parallel connected two induction motors drive, ISA Trans. 53 (2014) 1847–1856.

[5] M.A. Abbas, R. Christen, R. Christen, T.M. Jahns, Six-phase voltage source inverter driven induction motor, IEEE Trans. Ind. Appl. IA-20 (April (5)) (1984) 1251–1259.

[6] G.K. Singh, K. Nam, S.K. Lim, A simple indirect field-oriented control scheme for multiphase induction machine, IEEE Trans. Ind. Electron. 52 (4) (2005) 1177–1184.

[7] E. Levi, Multiphase electric machines for variable-speed applications, IEEE Trans. Ind. Electron. 55 (May) (2008) 1893–1909.

[8] A.R. Munoz,˜ T.A. Lipo, Dual stator winding induction machine drive, IEEE Trans.

[9] E. Levi, R. Bojoi, F. Profumo, H.A. Toliyat, S. Williamson, Multiphase induction motor drives—a technology status review, IET Electr.

[10] A.S. Abdel-Khalik, M.I. Masoud, S. Ahmed, A. Massoud, Calculation of derating factors based on steady-state unbalanced multiphase induction machine model under open phase(s) and optimal winding currents, Electr. Power Syst. Res. 106 (2014) 214–225.

[11] S.N. Vukosavic, M. Jones, E. Levi, D. Dujic, Experimental performance evaluation of a five-phase parallel-connected two-motor

[12] K. Matsuse, H. Kawai, Y. Kouno, J. Oikawa, Characteristics of speed sensorless vector controlled dual induction motor drive connected in parallel fed by a single inverter, IEEE Trans. Ind. Appl. 40 (1) (2004) 153–161.

[13] R. Gunabalan, V. Subbiah, Review of speed-sensorless vector control of parallel connected induction motor drive fed by a single inverter, JEE 12 (4) (2012) 73–82.

[14] K. Matsuse, Y. Kouno, H. Kawai, S. Yokomizo, A speed-sensorless vector control method of parallel-connected dual induction motor fed by a single inverter, IEEE Trans. Ind. Appl. 38 (6) (2002) 1566–1572.

[15] W. Ruxi, W. Yue, D. Qiang, H. Yanhui, Wang Zhaoan, Study of control methodology for single inverter parallel connected dual induction motors based on the dynamic model, in: Power Electronics Specialists Conference, 2006. PESC'06. 37th IEEE, 2006, pp. 1–7.

[16] J. Nishimura, K. Oka, K. Matsuse, A method of speed sensorless vector control of parallel-connected dual induction motors by a single inverter with a rotor flux control, in: Proceeding of ICEMS'07, Korea, 2007.

[17] R. Gunabalan, V. Subbiah, Speed-sensorless vector control of parallel connected induction motor drive with fuzzy controller, in: IEEE Inter. Conference on CICR'12, 2012.

[18] E.H. Mamdani, Application of fuzzy algorithms for control of simple dynamic plant, Proc. IEEE 121 (12) (1974) 1585–1588.

[19] W.Z. Qiao, M. Mizumoto, PID type fuzzy controller and parameters adaptive method, Fuzzy Sets Syst. 78 (1996) 23–35.

[20] M. Mizumoto, Product-sum-gravity method = fuzzy singleton-type reasoning method = simplified fuzzy reasoning method, in: Proceedings of the Fifth IEEE International Conference on Fuzzy Systems, vol. 3, 1996,pp. 2098–2102.

[21] Jang J.S.R., "ANFIS: Adaptive-network-based fuzzy inference systems", IEEE Transactions on systems, Man and Cybernetics, Vol.23, Issue.3, 1993, p. 665-685.

[22] J-S.R. Jang and C-T. Sun, "Neuro-Fuzzy Modeling and Control", Proceeding of the IEEE Transactions, Vol.83, No.3, pp.378-406, Mar 1995.